

See discussions, stats, and author profiles for this publication at: <https://www.researchgate.net/publication/278671530>

White Light Emitting Polymers from a Luminogen with Local Polarity Induced Enhanced Emission

ARTICLE *in* THE JOURNAL OF PHYSICAL CHEMISTRY C · NOVEMBER 2014

Impact Factor: 4.77 · DOI: 10.1021/jp5068439

CITATIONS

2

READS

26

5 AUTHORS, INCLUDING:



Ananthakrishnan Soundaram jeevarathinam

Western Kentucky University

14 PUBLICATIONS 36 CITATIONS

[SEE PROFILE](#)



E. Varathan

Central Leather Research Institute

16 PUBLICATIONS 46 CITATIONS

[SEE PROFILE](#)



N. Somanathan

Central Leather Research Institute

66 PUBLICATIONS 458 CITATIONS

[SEE PROFILE](#)



Asit Baran Mandal

Central Leather Research Institute

360 PUBLICATIONS 3,202 CITATIONS

[SEE PROFILE](#)

White Light Emitting Polymers from a Luminogen with Local Polarity Induced Enhanced Emission

Soundaram J. Ananthakrishnan,^{†,‡,§} E. Varathan,^{†,‡,§,||} V. Subramanian,^{†,‡,§,||} N. Somanathan,^{*,†,‡,§,||} and Asit B. Mandal^{*,†,‡,§,||}

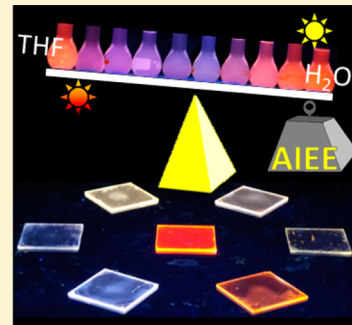
[†]CSIR-Network of Institutes for Solar Energy, New Delhi, India

^{||}Academy of Scientific and Innovative Research, New Delhi 110001, India

[§]Council of Scientific and Industrial Research (CSIR)-Central Leather Research Institute, Sardar Patel Road, Adyar, Chennai 600020, Tamil Nadu, India

Supporting Information

ABSTRACT: Aggregation induced enhanced emission (AIEE) is considered as an important tool to circumvent the aggregation caused quenching (ACQ) effect in organic light emitting diodes (OLEDs). Charge trapping and surplus long wavelength electroluminescence is a cause of concern in single polymer based white OLEDs. However, the potential of luminogens with AIEE property as a credible tool to offset the above problems in white light emitting single polymer is not properly explored. In this study design, synthesis and spectral characterization of a polymerizable luminogen, (2Z,2'Z)-6,6'-(2,7-dibromo-9H-fluorene-9,9-diyl)bis(hexane-6,1-diyl)bis(2-cyano-3-(10-hexyl-10H-phenothenothiazin-3-yl)acrylate(FCPA) with AIEE property and its copolymers is presented. Lippert-Mataga studies showed that reduced local polarity caused by aliphatic chains in condensed state of FCPA resulted in AIEE property. The copolymers P(FCPA-1) and P(FCPA-0.5) with 1% and 0.5% FCPA moieties showed white electroluminescence and enhanced thin film photoluminescence that matched very closely. The superior performance of OLEDs is attributed to the presence of a phenothiazine group in FCPA that resulted in nearly equal electron and hole injection barriers.



INTRODUCTION

Aggregation induced emission (AIE) and aggregation induced enhanced emission (AIEE) are deemed as effective tools for offsetting the low quantum yields of luminogens in solid state.^{1,2} Luminogens with AIE property showed very low or no emission in solution, while emission is turned on upon aggregation.³ AIEE luminogens, on the other hand, showed significant emission in solution that is enhanced upon aggregation.⁴ A survey of recent literature on AIE/AIEE luminogens revealed that they are sensitive to microenvironment.⁵ As a result, a myriad of applications have been successfully realized from these smart materials such as supersensitive explosive detection,⁶ sensors for heavy metals,⁷ thermofluorochromism,⁸ piezochromic or mechanochromic sensors,⁹ and organic light emitting diodes (OLEDs).¹⁰ However, OLED application is one of the most promising facets since AIE/AIEE luminogens can be highly emissive in thin films.

Long wavelength emitting AIE/AIEE fluorophores with color tunability are gaining importance since they can be used for undoped OLEDs and bioimaging applications.^{11–15} Particularly red emitting AIE molecules have been demonstrated for sensor and OLED applications.^{16,17} Phenothiazine is among the versatile building blocks for construction of luminogens with enhanced emission in solid state.¹⁸ It is evident from the recent literature that phenothiazine based building blocks have been

utilized for red emitting AIE luminogens.¹⁹ Further, phenothiazine was also used as a structural component in molecules with AIE property along with solvatochromic and piezochromic properties.²⁰ These properties were clearly ascribed to the actuation of a transition between twisted and planar conformations of these molecules by changes in microenvironment.^{18–20} The changes in the microenvironments can be brought about by external stimuli such as change in polarity of medium and physical stress. Thus, it is possible to tune the emission properties by precise control of the microenvironment of AIE fluorophores with phenothiazine moiety.²¹ The electron donating character in phenothiazine can be utilized to realize variety of spectral properties by versatile substitution in 3 and 7 positions.²²

The incorporation of phenothiazine in polymeric systems was found to impart reduced hole injection barrier and balanced charge carrier mobility due to the electron-rich nature of phenothiazine units.^{23–25} Copolymers of 10-alkylphenothiazine with fluorene have been explored with yellow or orange electroluminescence.²⁶

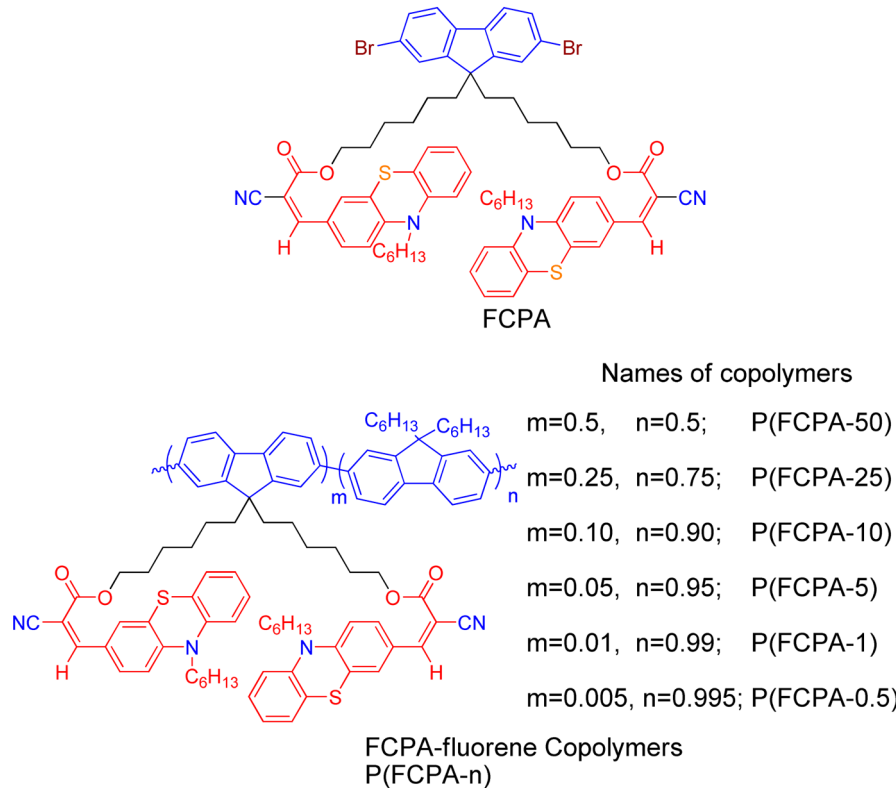
Single copolymers with white light emission have received seminal importance from researchers using various other

Received: July 9, 2014

Revised: November 10, 2014

Published: November 10, 2014

Chart 1. Structure of FCPA and FCPA-Fluorene Copolymers



structural components.²⁷ Charge trapping and consequent long wavelength emission have remained a challenge in achieving pure white electroluminescence in single polymer through conventional approach.^{27,28} Notwithstanding, the above developments, polyfluorenes have remained an integral part of these white emitting polymers with different covalent dopants in main chain and side chains of copolymers.²⁸ Studies on white light emitting polymers based on phenothiazine and other building blocks exhibited alteration of recombination zone- and field-dependent mobility leading to voltage-dependent electroluminescence.^{29–31} It is evident from the above discussions that the possibilities of using AIEE luminogen for white electroluminescent polymers were not explored properly.^{11–21}

Herein, we propose a strategy by using polymerizable red emitting AIEE fluorophore ($2Z,2'Z$)-6,6'-(2,7-dibromo-9H-fluorene-9,9-diyl)bis(hexane-6,1-diyl)bis(2-cyano-3-(10-hexyl-10H-phenothiazin-3-yl)acrylate (FCPA) as covalent dopant in white electroluminescent copolymers with six different compositions of FCPA (0.5, 1.0, 5.0, 10.0, 25.0, 50.0%). Using FCPA as polarizable monomer, different FCPA-fluorene copolymers having six different ratios of FCPA, namely, P(FCPA-0.5), P(FCPA-1), P(FCPA-5), P(FCPA-10), P(FCPA-25), and P(FCPA-50), were investigated for luminescence properties. The structures of FCPA and FCPA-fluorene copolymers are presented in Chart 1.

EXPERIMENTAL SECTION

Dynamic light scattering (DLS) of monomer and copolymers were performed on Malvern, dynamic light scattering instrument. Fluorescence lifetime analyses (FLT) were performed on IBH fluorescence lifetime instrument with 0.1 ns resolution. Data analyses of FLT data were performed using Horiba Jobin Yvon decay analysis program. Atomic force microscopy (AFM)

of thin films was recorded on Nova 1.0.26 RC1 atomic force microscope with NT-MDT solver software. Silicon cantilever (SII) with average frequency of 260–630 kHz with force constant of 28–91 N m⁻¹ were used in semicontact mode in AFM experiments. X-ray diffraction (XRD) data of monomer and copolymers were obtained using Bruker AXS D8 Advance X-ray diffractometer. Cu K α wavelength was used for XRD experiments. UV-visible absorbance was done on Varian Carey 50 Bio UV-visible spectrophotometer. Fluorescence spectra of monomer and copolymers were recorded on Varian Carey Eclipse fluorescence spectrophotometer. Cyclic voltammetry measurements were done using CHI 600D electrochemical workstation with platinum disc electrode as working electrode, Ag/AgCl electrode as reference electrode and platinum wire electrode as counter electrode. Measurements in cyclic voltammetry were performed by coating a thin layer of polymers on platinum disc electrode and measurements were performed in acetonitrile medium with tetrabutylammonium hexafluorophosphate as support electrolyte. OLEDs were fabricated by spin coating poly(3,4-ethylenedioxythiophene)/poly(styrenesulfonate) (PEDOT:PSS) on plasma cleaned indium tin (ITO) oxide substrate (thickness 110 nm, 10 Ω /square). The ITO plates coated with PEDOT:PSS were baked at 200 °C and then thin films of monomer and copolymers were spin coated from their respective chloroform solutions with 2 mg/mL concentration. Aluminum was deposited as cathode at 10⁻⁵ Torr. The luminescence–voltage ($L-V$) and Current–Voltage ($I-V$) characteristics were measured using Nucleonix type 60 PMT drawer assembly and Keithley 2400 source meter, respectively. The concentration of monomer used for spectroscopic, DLS, and FLT studies was 6.91×10^{-6} M, while that of polymers was 5×10^{-3} g dL⁻¹. Details of theoretical calculations are provided in Supporting Information.

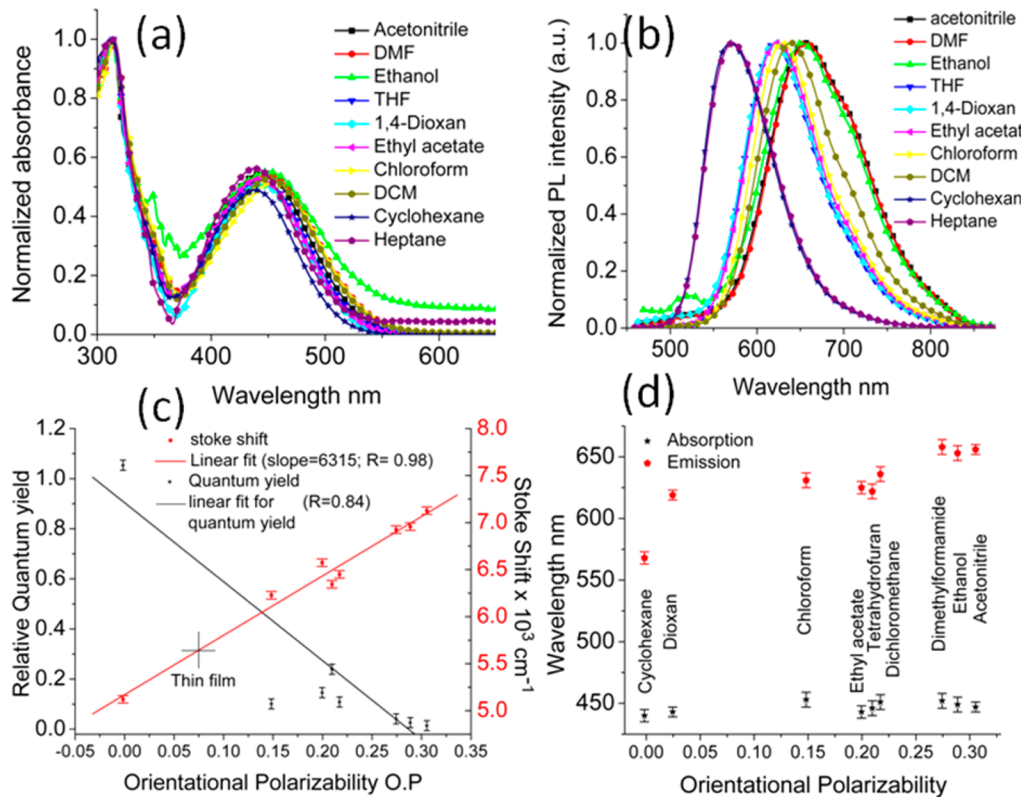


Figure 1. (a) Absorption, (b) photoluminescence (PL), (c) quantum yield and Lippert-Mataga plot of FCPA in different solvents, and (d) absorption and emission maxima of FCPA in different solvents.

RESULTS AND DISCUSSION

Spectral Properties of FCPA. The structure of polymerizable AIEE luminogen, FCPA (Chart 1) can be viewed as two phenothiazine dye units dangled to the termini of hexyl groups in 9,9-diethylfluorene through ester linkage.³² The solubility of FCPA in solvent with wide polarity range was helpful in complete characterization of the spectral and electronic properties. The absorption spectra of FCPA were recorded in different solvents, as presented in Figure 1.

The lowest energy absorption of FCPA observed at 440 nm in cyclohexane and at 453 nm in chloroform reveals the presence of intramolecular charge transfer (CT).³³ The CT band exhibited initial bathochromic shift followed by hypsochromic shift, characteristic of inverted solvatochromic character due to solvent-induced change of electronic structure in ground state (Figure 1).³⁴ The emission spectra of FCPA recorded in solvents with different polarity elicited a red shift from 568 to 658 nm with increase in polarity as observed for donor–acceptor systems.³⁵ The red shift in emission of FCPA in polar solvents (Figure 1) is attributed to the emission from solvent relaxed state. In addition to the above observation, Lippert-Mataga plot presented in Figure 1 showed a high slope implicit of a high transition dipole moment in FCPA. The photoluminescence quantum yield of FCPA showed a steady decrease with increase in solvent polarity (Figure 1). The reduced quantum yield indicate relaxation of excited state through torsional coordinates, thus, leading to twisted intramolecular charge transfer (TICT) state.^{35,36}

The thin films of FCPA elicited an intense red emission as shown in Figure 2 (photograph). Emission spectrum of FCPA in thin film elicited peak at 636 nm ($\varphi_f^{TF} = 37.5\%$, Table 1),

which is very close to the emission in dichloromethane signifying a similar microenvironment (local polarity).³⁷

Spectral Properties of Copolymers. The absorption and emission spectra of all copolymers in chloroform solution are presented in Figure 2. The absorption spectra of copolymers showed more characteristic absorption of poly(9,9-diethylfluorene)-2,7-diyl.³⁸ All copolymers except P(FCPA-50) did not exhibit the characteristic CT transition between 400 and 450 nm owing to low composition of FCPA units and relatively weak absorption coefficient of CT band (Table 1). The emission spectra of polymers in solution elicited a predominant emission at ~416 nm alongside low energy shoulders at ~435 and 466 nm characteristic of 9,9-diethylfluorene moiety.³⁸ Observed predominant blue emission can be attributed to high quantum yield of 9,9-diethylfluorene moiety in solution state and low quantum yield of FCPA in solution state (Table 1). In thin film, the absorption wavelength of copolymers was red-shifted to 380–390 nm, and the CT band observed in P(FCPA-50) copolymers merged with the high energy absorption due to broadening.

The emission spectra of the copolymers in thin film were completely different from that in the solution state. P(FCPA-50) copolymer exhibited a predominant emission at 611 nm in contrast to that of its solution emission, which can be attributed to an increase in quantum yield of FCPA in thin film state. Similarly, emission maxima of copolymers P(FCPA-25), P(FCPA-10), and P(FCPA-5) were observed at ~580 nm that is very close to emission of FCPA in cyclohexane and heptane, signifying a reduced local polarity due to alkyl groups present in 9,9-diethylfluorene units of copolymers. Thus, it can be concluded that the decreased local polarity in copolymers, P(FCPA-25), P(FCPA-10), and P(FCPA-5), results in

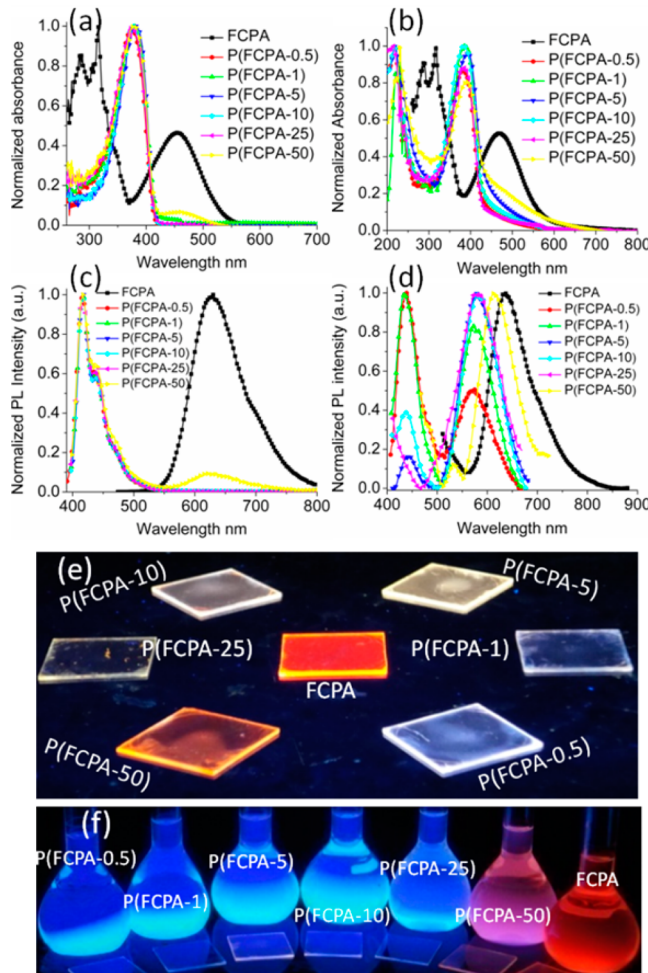


Figure 2. Absorption spectra in (a) solution, (b) thin film; PL spectra in (c) solution, (d) thin film of FCPA and copolymers; and (e) thin films and (f) chloroform solutions under irradiation at ~ 360 nm of copolymer and FCPA.

enhanced emission from FCPA units with consequently predominant emission at ~ 580 nm. In the case of P(FCPA-1) and P(FCPA-0.5) with very low composition of FCPA units, a weak emission at ~ 570 nm and stronger emission at ~ 436 nm resulted in white emission (Figure 2). The Commission Internationale de l'Eclairage (CIE) coordinates of P(FCPA-1) and P(FCPA-0.5) were found to be (0.31, 0.32) and (0.30, 0.33), respectively.

Aggregation-Induced Enhanced Emission (AIEE) Property of FCPA.

The monomer, FCPA, was studied for

AIEE property by measuring the emission properties of FCPA in THF–water mixtures of varying proportions.³⁹ Dynamic light scattering and fluorescence lifetime were also recorded simultaneously to understand the dynamics of emission and monitor the extent of aggregation in the THF–water mixtures (Figure 3).¹³ Emission of FCPA was initially observed at 624

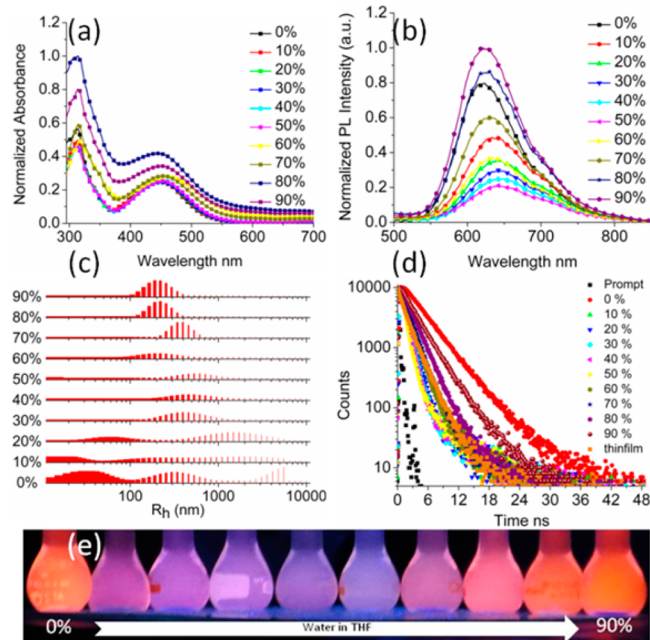


Figure 3. (a) Absorption, (b) PL spectra, (c) dynamic light scattering (DLS), (d) fluorescence lifetime (FLT), (e) photograph under irradiation at ~ 360 nm of FCPA in different THF–water mixtures.

nm in pure THF solution. When 10% of water was added to the solution of FCPA in THF, the emission was partially quenched and bathochromically shifted to 634 nm. A progressive bathochromic shift and quenching of emission was observed with increase in water content until the composition reached 40% with emission maximum at 647 nm. The corresponding dynamic light scattering (DLS) traces elicited a change from multimodal distribution in pure THF solution to unimodal distribution of hydrodynamic radii (R_h) at 40 and 50% water in THF.

The emission reached a minimum intensity at 50% water in THF mixture with a blue shift in the emission maximum to 642 nm. The quenching of emission of FCPA in THF–water mixtures with 10–50% composition of water was accompanied by appearance of ultrafast decay channel in fluorescence

Table 1. Spectral Properties of FCPA and Its Copolymers

polymer	$\lambda_{\text{abs}}^{\text{sol}}(\epsilon)^a$ (dL g ⁻¹ cm ⁻¹)	$\lambda_{\text{emi}}^{\text{sol}}(e)^b$ (nm)	$\lambda_{\text{abs}}^{\text{TF}}(e)^c$ (nm)	$\lambda_{\text{emi}}^{\text{TF}}(e)^d$ (nm)	$\Phi_{\text{PL}}^{\text{Sol}}(e)^e$ (%)	$\Phi_{\text{PL}}^{\text{TF}}(e)^f$ (%)
FCPA	454(1.41×10^6), 315(2.92×10^6), 284(2.56×10^6)	627	468, 318, 287	636	23.9 ^g	37.5
P(FCPA-0.5)	373(7.85×10^6)	467, 434, 416	382, 218	569, 436	59.0	59.4
P(FCPA-1)	378(8.04×10^6)	466, 435, 416	386, 222	573, 436	36.8	52.8
P(FCPA-5)	381(9.36×10^6)	465, 438, 416	393, 219	578, 443	47.2	51.9
P(FCPA-10)	378(6.47×10^6)	468, 438, 416	383, 217	581, 436	42.3	49.4
P(FCPA-25)	464(4.37×10^4), 375(5.86×10^6)	468, 439, 417	384, 214	580	28.1	48.6
P(FCPA-50)	458(4.45×10^5), 378(6.73×10^6)	630, 470, 438, 417	465, 390, 232	611	13.3	45.1

^a $\lambda_{\text{abs}}^{\text{sol}}$, absorption maxima in THF solution; ϵ , extinction coefficient. ^b $\lambda_{\text{emi}}^{\text{sol}}$, emission maxima in CHCl_3 solution. ^c $\lambda_{\text{abs}}^{\text{TF}}$, absorption maxima in thin film. ^d $\lambda_{\text{emi}}^{\text{TF}}$, emission maxima in thin film. ^e $\Phi_{\text{PL}}^{\text{Sol}}$, quantum yield in THF solution estimated using quinine sulfate standard (error $\pm 0.2\%$). ^f $\Phi_{\text{PL}}^{\text{TF}}$, absolute quantum yield in spun thin film in % (error $\pm 0.4\%$). ^gCalculated for THF solution by using Rhodamine 6G standard (error $\pm 0.2\%$).

lifetime and overall decrease in lifetime of emission (Figure 3 and Table 2). In a sharp contrast to the above observations,

Table 2. Fluorescence Lifetime Data of FCPA in Various Proportions of THF–Water Mixture

% water in THF	τ_1/τ_2^a (ns)	a_1/a_2^b (ns)	Φ_f^c (%)
0	8.1/2.2	2.8/97.1	23.9
10	5.2/0.9	4.3/95.7	4.9
20	5.6/0.7	4.9/95.0	3.6
30	5.0/6.4	7.6/92.4	3.1
40	4.6/0.6	9.5/90.5	2.5
50	3.7/0.5	14.5/85.5	2.3
60	4.2/0.9	6.0/94.0	2.9
70	4.5/1.0	3.5/96.5	4.6
80	6.9/1.3	1.6/98.4	45.3
90	3.48/1.62	10.4/89.6	61.1

^a τ_1/τ_2 , lifetime of decay channels 1 and 2 (standard error, 0; 1 ns).

^b a_1/a_2 , contribution of decay channels in % (error, $\pm 0.03\%$). ^c Φ_f , quantum yield calculated by using Rhodamine 6G standard (error, $\pm 0.2\%$).

emission intensity of FCPA increased with further increase in water content to 60% and a hypsochromic shift of emission to 634 nm was observed. The hypsochromic shift was progressively observed with increase in intensity as the water content in THF–water mixtures was increased. Maximum intensity of emission and a maximum blue shift to 622 nm was observed when the content of water in the mixtures was 90%. The corresponding DLS traces of a mixture with 60 to 90% water content showed a remarkable narrow distribution of size indicating formation of uniform sized aggregates.⁴⁰ Fluorescence lifetime of mixtures with high water content showed a disappearance of ultrafast decay component, indicating an increased radiative decay process.⁴¹ The increased quantum yield was observed at 90% water in THF mixture confirmed the presence of aggregation induced enhanced emission in FCPA (Table 2).⁴² The quenching with red shift of emission of FCPA in mixtures with 10–40% of water in THF is attributed to increased polarity of medium.⁴³ Enhancement in emission and hypsochromic shift in mixtures with 60–90% composition of water is due to the formation of aggregates with hydrophobic

alkyl chains forming the core that resulted in low polarity.^{37,44} Thus, a low local polarity in aggregates caused by aliphatic chains present in the polymers actuated the AIEE property of FCPA in contrast to restricted intramolecular rotation (RIR) and aggregation induced planarization mechanisms, as observed in most of the reported systems.^{3,43,45}

To gain more insight on the nature of transitions in FCPA, frontier molecular orbital (FMO) distributions were studied using density functional theory (DFT) at the B3LYP/6-31G* level in different solvents using the polarized continuum model (PCM). Figure 4 presents the optimized geometry of FCPA in hexane and acetonitrile with the FMO distributions indicating a “bow and arrow like” geometry of FCPA with the phenothiazine units perpendicular to the plane of the fluorene ring. The optimized ground state geometries did not show much variation as the solvent polarity was changed. The HOMO of FCPA is localized on the phenothiazine unit, while the LUMO is localized on cyanoacetate moiety, indicating the presence of intramolecular charge transfer between donor (phenothiazine) to acceptor (cyanoacetate moiety). TD-DFT calculations indicated that the low energy band constitutes transitions from HOMO → LUMO+1 (50%) and HOMO-1 → LUMO (47%; Table S3, Supporting Information). The corresponding FMO distribution showed that HOMO-1 and HOMO were localized on phenothiazine moiety, while LUMO and LUMO+1 were localized on the cyanoacetate moiety. All absorption bands calculated using TD-DFT calculations closely matched with that of the experimental values. The near-linear dependence of the stoke’s shift, as observed in the Lippert-Mataga study, and the charge transfer nature of the low energy transition clearly showed that the stoke shifts were a direct consequence of alteration of relative energies of the local excited (LE) state and charge transfer (CT) state.⁴⁶ The change in the dipole moment from the Lippert-Mataga study clearly indicates a charge transfer transition between ground state with a dipole of (μ_g) 11.3 D and excited state with a dipole moment (μ_e) of 20.4 D.^{44,47} The calculated change in the dipole from the Lippert-Mataga study showed that the change in dipole moment ($\Delta\mu$) to be 9.1 D calculated with onsagar cavity radius (a) of 7.90 Å. Further, the observed stoke shift in thin film (Figure 1c) showed that the local polarity also decreased in the

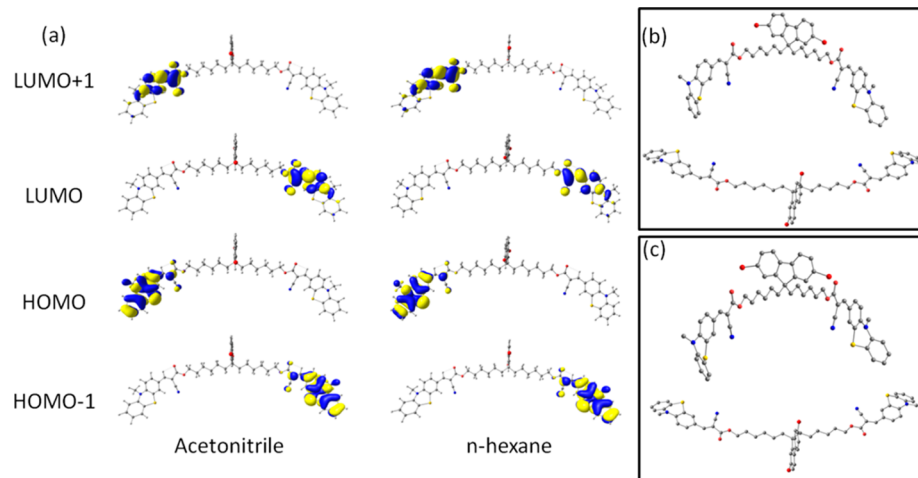


Figure 4. (a) Topologies of frontier molecular orbitals (isosurface value = 0.025 au) of FCPA calculated at the B3LYP/6-31G* level in solution using a PCM model; lateral (above) and top views (below) of FCPA geometry optimized in (b) acetonitrile and (c) *n*-hexane. The hydrogen atoms are omitted here for clarity.

condensed state due to nonpolar chains present in the FCPA structure. Hence, the observed increase in the quantum yield can be attributed to the decreased local polarity in thin film state which is very similar to a situation in low polarity solvent with increased probability of radiative decay process.⁴⁸

AIEE Property in Copolymers. Owing to the AIEE property of FCPA, the polymers were also studied for the same. Enhanced emission was observed in the case of P(FCPA-50) copolymer with maximum intensity of emission observed with 70% water in THF. However, the emission wavelength was completely shifted from 416 to 616 nm (Figure 5) signifying an

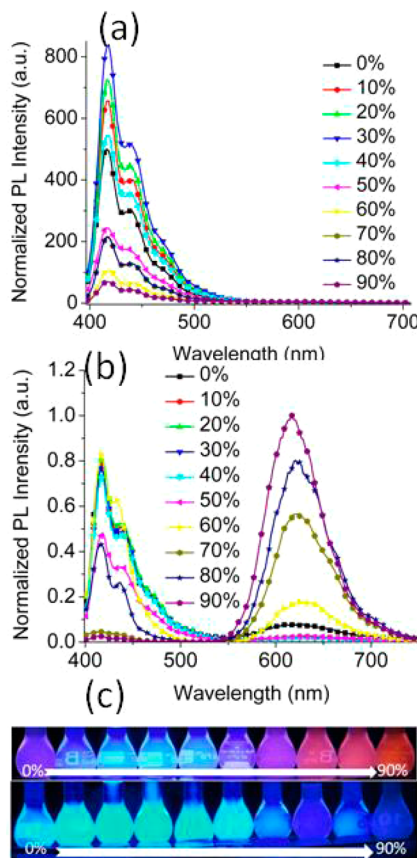


Figure 5. PL spectra of (a) P(FCPA-25) and (b) P(FCPA-50); Photograph of (c) P(FCPA-50) (above) and P(FCPA-25) (below) under irradiation at ~ 360 nm in different THF–water mixtures.

effective quenching of blue emission from dihexylfluorene moieties and enhancement of red emission from FCPA units present in the polymer. The double fluorescence phenomenon is clearly visible in P(FCPA-50) due to relatively high composition of FCPA units. However, it is interesting to note that the P(FCPA-25) copolymer elicited a maximum intensity emission at 30% water in THF (Figure 5) and steadily showed a decrease until it slightly enhanced at 70% water content was observed. The above observation can be attributed to the formation of random amorphous aggregates in 70% water–THF mixture that lead to precipitation of polymer.⁴⁹ Other polymers did not show enhancement of emission upon aggregation owing to low composition of FCPA.⁵⁰ Further the emission property of the polymers with 0.5–25% content of FCPA showed emission spectra in aggregates to be identical to that in respective solutions. The above observation can be related to strong solvent–solute interactions. Nevertheless, it is

interesting to note the emission spectra of copolymers in thin film are completely different from the aggregates. The thin films of polymers spin coated on quartz substrates exhibited higher quantum yield than the respective solutions.

The fluorescence lifetime data presented in Table 3 from solution and thin film indicate a longer average lifetime for thin

Table 3. Fluorescence Lifetime Data of Copolymers in Solution and Thin Film

monomer/polymer	fluorescence lifetime	
	τ_1/τ_2^a (ns) (a_1/a_2 ; %)	τ_1/τ_2^b (ns) (a_1/a_2 ; %)
FCPA	8.1/2.2 (2.8/97.1)	3.3/1.7 (2.6/65.4)
P(FCPA-0.5)	3.8/0.6 (2.0/98.0)	7.3/0.2 (1.4/98.6)
P(FCPA-1)	3.9/5.5 (1.9/98.1)	5.3/0.2 (3.0/97.0)
P(FCPA-5)	3.2/0.5 (2.8/97.2)	5.0/1.8 (41.1/58.9)
P(FCPA-10)	4.0/0.6 (2.1/97.9)	4.6/1.5 (40.5/59.5)
P(FCPA-25)	3.0/0.6 (2.0/98.0)	4.1/1.8 (2.0/98.0)
P(FCPA-50)	4.9/2.2 (6.2/93.8)	2.6/1.0 (59.5/40.5)

^a τ_1/τ_2 , lifetime of decay channels 1 and 2 (standard error, 0; 1 ns) and a_1/a_2 , contribution of decay channels in % for solution state (error, $\pm 0.3\%$). ^b T_1/T_2 , lifetime of decay channels 1–3 (standard error, 0.1 ns) and A_1/A_2 , contribution of different decay channel in % for thin films (error, $\pm 0.3\%$).

films, indicating the presence of a dominant radiative decay process. Thus, the presence of FCPA in small proportions resulted in decreased π – π interaction in copolymers. FCPA with AIEE property was thus used for white emission with a high quantum yield in P(FCPA-1) and P(FCPA-0.5). White emission using AIE luminogen as comonomer in a single polymer is highly desirable but is seldom reported until date. Here the local polarity induced hypsochromic shift of FCPA emission toward orange emission and consequent enhancement of quantum yield was used to generate white light emission by complementary color mixing.

Morphology and Intermolecular Interaction. The monomer FCPA and the copolymers were studied using X-ray diffraction analysis (XRD) and atomic force microscopy (AFM) to understand the intermolecular interactions. A comparison of copolymers by their morphology and XRD diffraction patterns revealed that the change in composition of FCPA units had a strong effect on the intermolecular interactions. FCPA did not show any peak in XRD, suggesting that FCPA is completely amorphous (Figure 6).⁵¹ The differential scanning calorimetry (DSC) of FCPA (Figure S13, Supporting Information) revealed that the melting point of FCPA was 48.7 °C and the absence of the crystallization peak on the cooling cycle indicated that the compound is amorphous and explained its film-forming property. This observation is in contrast to the previous AIE molecules reported with phenothiazine and bulky aromatic groups.⁵² AFM micrograph of FCPA did not elicit any significant morphological features and hence confirm the amorphous nature.

The copolymers on the other hand exhibited XRD patterns that are very similar to that of dialkyl fluorene that changed progressively with the increase in composition of FCPA. For example the copolymer, P(FCPA-0.5) showed a reflection at 6.77° 2θ corresponding to the β -phase of dialkylfluorene; however, the peak was not clearly observed in the case of P(FCPA-25) and P(FCPA-50) copolymers.⁵³ The reflection corresponding to the β -phase formation in the copolymers

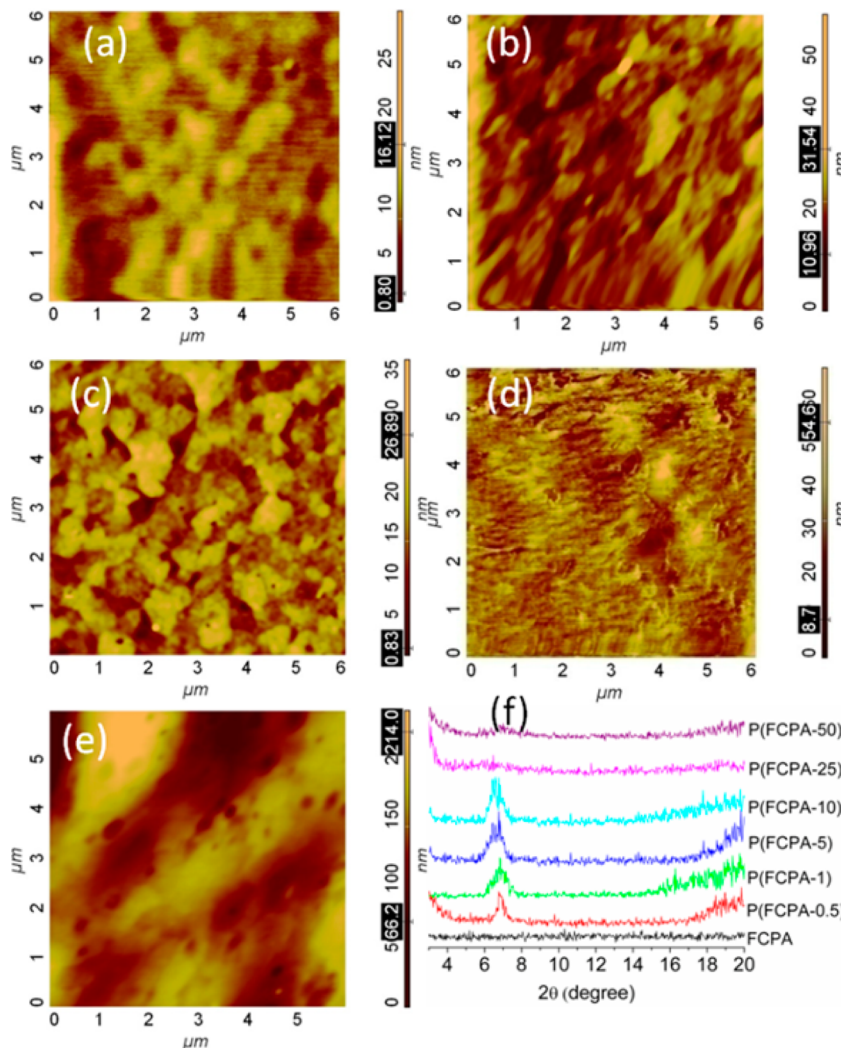


Figure 6. AFM micrographs of (a) FCPA, (b) P(FCPA-0.5), (c) P(FCPA-10), (d) P(FCPA-25), (e) P(FCPA-50), and (f) X-ray diffraction (XRD) traces of copolymers.

correspond to the distance of 13.04 \AA , which is very close to that observed for poly(9,9-dihexylfluorene) systems.⁵³ In addition to the above reflection, a broad peak with onset at around 16.79° 2θ corresponds to the amorphous halo that is characteristic of amorphous phase present in dialkyl fluorene polymers.⁵⁴ The XRD patterns of P(FCPA-25) and P(FCPA-50) showed very weak reflections that was not clearly observable signified a similarity to pure FCPA film in with amorphous nature.⁵⁵

AFM micrograph of the copolymers showed a progressive change from P(FCPA-0.5) with more lamellae like structures to terraced morphology in P(FCPA-10). As the composition of FCPA units further increased in P(FCPA-25) and P(FCPA-50), the AFM morphology change to fibrillar and amorphous, respectively.⁵⁵

OLED Device Characteristics of Monomer and Copolymers. The monomer, FCPA, and the copolymers were used to fabricate OLEDs with device configuration of ITO/PEDOT:PSS/polymer/Al by solution processing. OLEDs of polymers elicited a broad electroluminescence spectrum that had same spectral width as the corresponding PL spectra. The EL spectrum of FCPA was observed to be wider than the PL spectrum which can be attributed to the formation of

electromer/excimer.⁵⁶ Further the energy level diagram presented in Figure 7 show that the electron injection barrier for FCPA is 0.63 eV and hole injection barrier was found to be 0.46 eV . Hence, FCPA would constitute holes as majority charge carriers leading to imbalance in charge injection. However, the 9,9-dihexylfluorene backbone has a lowest unoccupied molecular orbital (LUMO) and highest occupied molecular orbital (HOMO) value of ~ -2.37 and $\sim -5.5 \text{ eV}$;

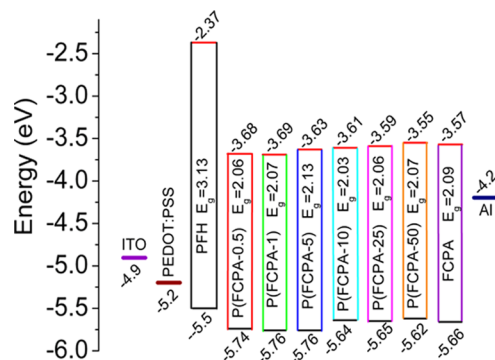


Figure 7. Energy level diagram of FCPA and copolymers.

hence, FCPA can be expected to act as a trap for electrons.^{27,28} The copolymers with low composition of FCPA units, namely, P(FCPA-0.5) and P(FCPA-1), showed a hybrid character of energy levels that is intermediate between dialkylfluorene and FCPA monomer. Thus, P(FCPA-0.5) and P(FCPA-1) elicited LUMO levels close to that of FCPA monomer.

It is evident from Figure 7 that the LUMO energy level of P(FCPA-0.5) and P(FCPA-1) were -3.68 and -3.69 eV, respectively, while the HOMO levels were found to be -5.74 and 5.76 eV, respectively. Electron and hole injection barrier values from Figure 7 was found to be 0.52 and 0.54 eV respectively for P(FCPA-0.5), while P(FCPA-1) also showed almost same values. The above injection barrier values for hole and electrons in case of P(FCPA-0.5) and P(FCPA-1) are almost equal. The above observation clearly points to a balanced charge carrier injection and recombination which is also supported by nearly same wavelength of PL and EL for these polymers.⁵⁷ The absence of surplus long wavelength emission in electroluminescence, as observed previously for some white light emitting single polymers, can be attributed to ambipolar charge injection.⁵⁷ It can also be observed that the EL spectrum of P(FCPA-0.5) with white light emission is unchanged upon change in voltage (Figure 8). The maximum

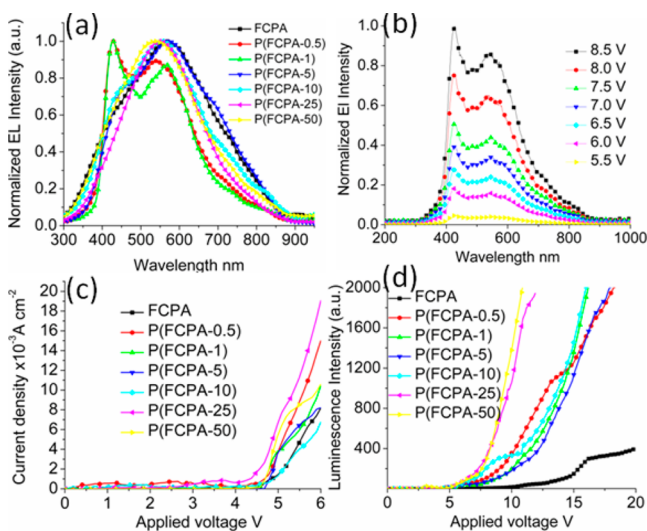


Figure 8. (a) Electroluminescence spectra of monomer and copolymers at 10 V, (b) EL spectra of P(FCPA-0.5) in different applied voltage, (c) luminescence-voltage, and (d) current-voltage characteristics.

brightness of the white OLEDs fabricated from P(FCPA-0.5) and P(FCPA-1) were found to be 5862 and 6184 cd/m^2 , respectively. CIE coordinates of the above two copolymers in EL was found to be $0.30, 0.33$ and $0.31, 0.32$, respectively, that closely correspond to the pure white light emission. The luminous efficiency of the OLEDs with P(FCPA-0.5) and P(FCPA-1) were found to be 4.6 and 4.5 lm/W (Table S2). Thus, the copolymers constitute a unique class of single white light emitting polymers with covalently linked AIEE luminogen. The copolymers with higher compositions of FCPA in the backbone also exhibited near white light with P(FCPA-5) showing a CIE coordinate of $0.34, 0.45$ and P(FCPA-10) with $0.38, 0.40$. The CIE coordinates of EL from P(FCPA-10) and P(FCPA-5) closely correspond to white light emission from single polymers reported previously.⁵⁸ FCPA, P(FCPA-25), and P(FCPA-50) exhibited red, yellow, and orange electro-

luminescence; however, the performance of the LEDs was lower than that of P(FCPA-0.5) and P(FCPA-1) copolymers due to imbalance in charge injection (Table S2). All the copolymers and monomer elicited a turn on voltage of 5 V (Figure 8) and ambipolar charge carrier mobilities measured by space charge limited current was also found to be higher for P(FCPA-0.5) and P(FCPA-1) compared to other polymers (Table S2, Supporting Information).

Calculation of Charge Carrier Mobilities of Copolymers. In organic electronic materials, charge motion occurs predominantly by a hopping-type mechanism where charge transport property described by the incoherent hopping model,⁵⁹ by means of standard Marcus equation⁶⁰ governed by reorganization energy. It is clear from the Marcus equation, the charge transfer rate depends on two key parameters, the charge transfer integral (coupling matrix) and reorganization energy. The experimentally determined coupling matrix for organic molecules is, however, reported to be rather narrow. Hence, one can assume that the charge (hole and electron) mobility of the model oligomer will be dominated by the respective reorganization energies, although such an assumption would be too simplistic. However, such an assumption is widely used to calculate the charge mobility of oligomer and organic molecules.^{61–65} The reorganization energies were evaluated by the adiabatic potential-energy surface approach described in detail in previous studies.^{64,65} In order to evaluate the charge mobility, the reorganization energies of the oligomer were evaluated. According to Marcus–Hush theory, the low reorganization energies are associated with a higher transport rate of the carriers. The calculated hole (λ_h) and electron (λ_e) reorganization energies of FCPA is displayed in Table 4. From

Table 4. Calculated Hole (λ_h) and Electron (λ_e) Reorganization Energies of FCPA at B3LYP/6-31G* Level (Energies in eV)

compound	hole			electron			
	FCPA	λ_1	λ_2	λ_h	λ_3	λ_4	λ_e
FCPA		0.06	0.06	0.12	0.12	0.10	0.22

Table 4, it can be seen that the balanced charge transport is found in FCPA as the reorganization energies for their λ_h and λ_e are comparable ($\Delta\lambda = 0.10 \text{ eV}$), which is sufficient⁶⁵ for them to act as a ambipolar material.

CONCLUSIONS

A polymerizable red emitting monomer with phenothiazine based donor–acceptor system was designed with AIEE property. The AIEE monomer is unique since its AIEE property is attributed to the local polarity of donor–acceptor system in condensed state. Reports with AIEE actuated exclusively by local polarity alone are relatively very rare.⁴⁴ Most of the systems with AIEE property relied on restricted intermolecular rotation as a principle way to trigger the property. The actuation of AIEE in FCPA by low polarity is evident from the hypsochromic shift of PL emission maxima in thin films relative to that in polar solvents. FCPA-fluorene copolymers with different ratios of FCPA were demonstrated to tune the quality of white light in OLEDs. Further, the copolymers P(FCPA-0.5) and P(FCPA-1) elicited a minimized charge carrier trapping resulting in stable electroluminescence. To date the polymer systems with even best efficiency in OLEDs were found to suffer from charge trapping and

consequent surplus long wavelength emission.⁶⁶ Thus, the copolymers presented in this study were demonstrated to successfully offset the above problems with balanced charge injection barriers.

■ ASSOCIATED CONTENT

Supporting Information

Detailed synthetic procedure of intermediate compounds, ¹H and ¹³C NMR and MALDI mass spectra of all intermediates, FCPA, and copolymers, and details of the theoretical calculations. This material is available free of charge via the Internet at <http://pubs.acs.org>.

■ AUTHOR INFORMATION

Corresponding Authors

*E-mail: nsomanathan@rediffmail.com. Phone: +91-44-24437189.

*E-mail: abmandal@hotmail.com. Phone: +91-44-24910846.

Author Contributions

[†]All authors contributed equally.

Notes

The authors declare no competing financial interest.

■ ACKNOWLEDGMENTS

Timely help from Prof. R. Damodaran and Mr. E. Ramachandran is gratefully acknowledged. The authors thank Dr. A. Ajayaghosh, Dr. J. D. Sudha, and Mr. R. Ramakrishnan, NIIST, Trivandrum for help in recording AFM, fluorescence lifetime studies, and dynamic light scattering. The authors sincerely thank Council of Scientific and Industrial Research (CSIR), India, for financial support through funds of NWP-55. One of the authors, Ananthakrishnan, S. J., thanks CSIR, India, for financial support through Senior Research Fellowship (Grant No. 31/6(0340)/2010-EMR-I).

■ REFERENCES

- (1) (a) Luo, J.; Xie, Z.; Lam, J. W. Y.; Cheng, L.; Chen, H.; Qiu, C.; Kwok, H. S.; Zhan, X.; Liu, Y.; Zhu, D.; et al. Aggregation-Induced Emission of 1-Methyl-1,2,3,4,5-pentaphenylsilole. *Chem. Commun.* **2001**, 1740–1741.
- (2) Chen, J.; Xu, B.; Ouyang, X.; Tang, B. Z.; Cao, Y. Aggregation-Induced Emission of *cis,cis*-1,2,3,4-Tetraphenylbutadiene from Restricted Intramolecular Rotation. *J. Phys. Chem. A* **2004**, *108*, 7522–7526.
- (3) Hong, Y.; Lam, J. W. Y.; Tang, B. Z. Aggregation-Induced Emission. *Chem. Soc. Rev.* **2011**, *40*, 5361–5388.
- (4) Huang, W.; Tang, F.; Li, B.; Sua, J.; Tian, H. Large Cyano- and Triazine-substituted D-π-A-π-D Structures as Efficient AIEE Solid Emitters with Large Two-Photon Absorption Crossections. *J. Mater. Chem. C* **2014**, *2*, 1141–1148.
- (5) Hong, Y.; Lam, J. W. Y.; Tang, B. Z. Aggregation-Induced Emission: Phenomenon, Mechanism and Applications. *Chem. Commun.* **2009**, 4332–4353.
- (6) Vij, V.; Bhalla, V.; Kumar, M. Attogram Detection of Picric Acid by Hexa-peri-Hexabenzocoronene-Based Chemosensors by Controlled Aggregation-Induced Emission Enhancement. *ACS Appl. Mater. Interfaces* **2013**, *5*, 5373–5380.
- (7) Mukherjee, S.; Thilagar, P. Molecular Flexibility Tuned Emission in "V" Shaped Naphthalimides: Hg(II) Detection and Aggregation-Induced Emission Enhancement (AIEE). *Chem. Commun.* **2013**, *49*, 7292–7294.
- (8) Wei, R.; Song, P.; Tong, A. Reversible Thermochromism of Aggregation-Induced Emission-Active Benzophenone Azine Based on Polymorph-Dependent Excited-State Intramolecular Proton Transfer Fluorescence. *J. Phys. Chem. C* **2013**, *117*, 3467–3474.
- (9) Shen, X. Y.; Wang, Y. J.; Zhao, E.; Yuan, W. Z.; Liu, Y.; Lu, P.; Qin, A.; Ma, Y.; Sun, J. Z.; Tang, B. Z. Largely Blue-Shifted Emission Through Minor Structural Modifications: Molecular Design, Synthesis, Aggregation-Induced Emission and Deep-Blue OLED Application. *J. Phys. Chem. C* **2013**, *117*, 7334–7347.
- (10) Huang, J.; Sun, N.; Chen, P.; Tang, R.; Li, Q.; Ma, D.; Li, Z. Largely Blue-shifted Emission through Minor Structural Modifications: Molecular Design, Synthesis, Aggregation-Induced Emission and Deep-Blue OLED Application. *Chem. Commun.* **2014**, *50*, 2136–2138.
- (11) Niu, C.; Zhao, L.; Fang, T.; Deng, X.; Ma, H.; Zhang, J.; Na, N.; Han, J.; Ouyang, J. Color- and Morphology-Controlled Self-Assembly of New Electron-Donor Substituted Aggregation-Induced Emission Compounds. *Langumir* **2014**, *30*, 2351–2359.
- (12) Li, K.; Qin, W.; Ding, D.; Tomczak, N.; Geng, J.; Liu, R.; Liu, J.; Zhang, X.; Liu, H.; Liu, B.; et al. Photostable Fluorescent Organic Dots with Aggregation-Induced Emission (AIE Dots) for Noninvasive Long-Term Cell Tracing. *Sci. Rep.* **2013**, *3*, 1150.
- (13) Ananthakrishnan, S. J.; Varathan, E.; Ravindran, E.; Somanathan, N.; Subramanian, V.; Mandal, A. B.; Sudha, J. D.; Ramakrishnan, R. A Solution Processable Fluorene–Fluorenone Oligomer with Aggregation Induced Emission Enhancement. *Chem. Commun.* **2013**, *49*, 10742–10744.
- (14) Geng, J.; Zhu, Z.; Qin, W.; Ma, L.; Hu, Y.; Gurzadyan, G. G.; Tang, B. Z.; Liu, B. Near-Infrared Fluorescence Amplified Organic Nanoparticles With Aggregation-Induced Emission Characteristics for In Vivo Imaging. *Nanoscale* **2014**, *6*, 939–945.
- (15) Du, X.; Qi, J.; Zhang, Z.; Ma, D.; Wang, Z. Y. Efficient Non-Doped Near Infrared Organic Light-Emitting Devices Based on Fluorophores with Aggregation-induced Emission Enhancement. *Chem. Mater.* **2012**, *24*, 2178–2185.
- (16) Chen, S.; Liu, J.; Liu, Y.; Su, H.; Hong, Y.; Jim, C. K. W.; Kwok, R. T. K.; Zhao, N.; Qin, W.; Lam, J. W. Y.; et al. An AIE-active Hemicyanine Fluorogen with Stimuli-Responsive Red/Blue Emission: Extending the pH Sensing Range by "Switch + Knob" Effect. *Chem. Sci.* **2012**, *3*, 1804–1809.
- (17) Ning, Z.; Chen, Z.; Zhang, Q.; Yan, Y.; Qian, S.; Cao, Y.; Tian, H. Aggregation-Induced Emission (AIE)-Active Starburst Triarylamine Fluorophores as Potential Non-Doped Red Emitters for Organic Light-Emitting Diodes and Cl₂ Gas Chemodosimeter. *Adv. Funct. Mater.* **2007**, *17*, 3799–3807.
- (18) Wang, B.; Wang, Y.; Hua, J.; Jiang, Y.; Huang, J.; Qian, S.; Tian, H. Starburst Triarylamine Donor–Acceptor–Donor Quadrupolar Derivatives Based on Cyano-Substituted Diphenylaminostyrylbenzene: Tunable Aggregation-Induced Emission Colors and Large Two-Photon Absorption Cross Sections. *Chem.—Eur. J.* **2011**, *17*, 2647–2655.
- (19) Zhang, J.; Xu, B.; Chen, J.; Wang, L.; Tian, W. Oligo(phenothiazine)s: Twisted Intramolecular Charge Transfer and Aggregation-Induced Emission. *J. Phys. Chem. C* **2013**, *117*, 23117–23125.
- (20) Zhang, X.; Chi, Z.; Zhang, J.; Li, H.; Xu, B.; Li, X.; Liu, S.; Zhang, Y.; Xu, J. Piezofluorochromic Properties and Mechanism of an Aggregation-Induced Emission Enhancement Compound Containing N-Hexyl-phenothiazine and Anthracene Moieties. *J. Phys. Chem. B* **2011**, *115*, 7606–7611.
- (21) Yang, X.; Lu, R.; Zhou, H.; Xue, P.; Wang, F.; Chen, P.; Zhao, Y. Aggregation-Induced Blue Shift of Fluorescence Emission Due to Suppression of TICT in a Phenothiazine-Based Organogel. *J. Colloid Interface Sci.* **2009**, *339*, 527–532.
- (22) Li, D.; Lv, L.; Sun, P.; Zhou, W.; Wang, P.; Wu, J.; Kan, Y.; Zhou, H.; Tian, Y. The Facile Synthesis of Novel Phenothiazine Derivatives for Blue, Yellow-Green, and Red Light Emission. *Dyes Pigm.* **2009**, *83*, 180–186.
- (23) Elkassih, S. A.; Sista, P.; Magurudeniya, H. D.; Papadimitratos, A.; Zakhidov, A. A.; Biewer, M. C.; Stefan, M. C. Phenothiazine Semiconducting Polymer for Light-Emitting Diodes. *Macromol. Chem. Phys.* **2013**, *214*, 572–577.
- (24) Hwang, D.-H.; Kim, S.-K.; Park, M.-J.; Lee, J.-H.; Koo, B.-W.; Kang, I.-N.; Kim, S.-H.; Zyung, T. Conjugated Polymers Based on

- Phenothiazine and Fluorene in Light-Emitting Diodes and Field Effect Transistors. *Chem. Mater.* **2004**, *16*, 1298–1303.
- (25) Park, Y.; Kim, B.; Lee, C.; Hyun, A.; Jang, S.; Lee, J.-H.; Gal, Y.-S.; Kim, T. H.; Kim, K.-S.; Park, J. Highly Efficient New Hole Injection Materials for OLEDs Based on Dimeric Phenothiazine and Phenoxyazine Derivatives. *J. Phys. Chem. C* **2011**, *115*, 4843–4850.
- (26) Kulkarni, A. P.; Kong, X.; Jenekhe, S. A. Polyfluorene Terpolymers Containing Phenothiazine and Fluorenone: Effects of Donor and Acceptor Moieties on Energy and Intrachain Charge Transfer Processes in the Photoluminescence and Electroluminescence of Multichromophore Copolymers. *Macromolecules* **2006**, *39*, 8699–8711.
- (27) Liu, J.; Zhou, Q.; Cheng, Y.; Geng, Y.; Wang, L.; Ma, D.; Jing, X.; Wang, F. The First Single Polymer with Simultaneous Blue, Green, and Red Emission for White Electroluminescence. *Adv. Mater.* **2005**, *17*, 2974–2978.
- (28) Chuang, C.-Y.; Shih, P.-I.; Chien, C.-H.; Wu, F.-I.; Shu, C.-F. Bright-White Light-Emitting Devices Based on a Single Polymer Exhibiting Simultaneous Blue, Green, and Red Emissions. *Macromolecules* **2007**, *40*, 247–252.
- (29) Park, M.-J.; Lee, J.; Park, J.-H.; Lee, S. K.; Lee, J.-I.; Chu, H.-Y.; Hwang, D.-H.; Shim, H.-K. Synthesis, Characterization, and Electroluminescence of Polyfluorene Copolymers with Phenothiazine Derivative; Their Applications to High-Efficiency Red and White PLEDs. *Macromolecules* **2008**, *41*, 9643–9649.
- (30) Park, M.-J.; Lee, J.; Park, J.-H.; Lee, S. K.; Lee, J.-I.; Chu, H.-Y.; Hwang, D.-H.; Shim, H.-K. Synthesis and Electroluminescence of New Polyfluorene Copolymers with Phenothiazine Derivative. Their Application in White-Light-Emitting Diodes. *Macromolecules* **2008**, *41*, 3063–3070.
- (31) Chen, S.; Wu, Q.; Kong, M.; Zhao, X.; Yu, Z.; Jia, P.; Huang, W. On the Origin of the Shift in Color in White Organic Light-Emitting Diodes. *J. Mater. Chem. C* **2013**, *1*, 3508–3524.
- (32) Yang, C.-J.; Chang, Y. J.; Watanabe, M.; Hon, Y.-S.; Chow, T. J. Phenothiazine Derivatives as Organic Sensitizers for Highly Efficient Dye-Sensitized Solar Cells. *J. Mater. Chem.* **2012**, *22*, 4040–4049.
- (33) Agrawal, S.; Pastore, M.; Marotta, G.; Reddy, M. A.; Chandrasekharan, M.; De Angelis, F. Optical Properties and Aggregation of Phenothiazine-Based Dye-Sensitizers for Solar Cells Applications: A Combined Experimental and Computational Investigation. *J. Phys. Chem. C* **2013**, *117*, 9613–9622.
- (34) Reichardt, C. Solvatochromic Dyes as Solvent Polarity Indicators. *Chem. Rev.* **1994**, *94*, 2319–2358.
- (35) Shen, X. Y.; Yuan, W. Z.; Liu, Y.; Zhao, Q.; Lu, P.; Ma, Y.; Williams, I. D.; Qin, A.; Sun, J. Z.; Tang, B. Z. Fumaronitrile-Based Fluorogen: Red to Near-infrared Fluorescence, Aggregation-Induced Emission, Solvatochromism, and Twisted Intramolecular Charge Transfer. *J. Phys. Chem. C* **2012**, *116*, 10541–10547.
- (36) Virgili, T.; Forni, A.; Cariati, E.; Pasini, D.; Botta, C. Direct Evidence of Torsional Motion in an Aggregation-Induced Emissive Chromophore. *J. Phys. Chem. C* **2013**, *117*, 27161–27166.
- (37) Morris, C.; Szczupak, B.; Klymchenko, A. S.; Ryder, A. G. Study of Water Adsorption in Poly(*N*-isopropylacrylamide) Thin Films Using Fluorescence Emission of 3-Hydroxyflavone Probes. *Macromolecules* **2010**, *43*, 9488–9494.
- (38) Su, F.-K.; Hong, J.-L.; Lin, L.-L. Restraining the Aggregation of Poly(9,9-dihexylfluorene) by Crosslinked Poly(methyl methacrylate) Networks. *J. Appl. Polym. Sci.* **2007**, *106*, 3308–3314.
- (39) Feng, H.-T.; Song, S.; Chen, Y.-C.; Shenb, C.-H.; Zheng, Y.-S. Self-Assembled Tetraphenylethylene Macrocycle Nanofibrous Materials for the Visual Detection of Copper(II) in Water. *J. Mater. Chem. C* **2014**, *2*, 2353–2359.
- (40) Zhang, G.; Jiang, M.; Chi, W. Intermacromolecular Complexation due to Specific Interactions, 14. The Chain Architectural Effect of Block Ionomers on Complexation. *Macromol. Chem. Phys.* **2001**, *202*, 1750–1756.
- (41) Ren, Y.; Lam, J. W. Y.; Dong, Y.; Tang, B. Z.; Wong, K. S. Enhanced Emission Efficiency and Excited State Lifetime due to Restricted Intramolecular Motion in Silole Aggregates. *J. Phys. Chem. B* **2005**, *109*, 1135–1140.
- (42) Boominathan, M.; Sathish, V.; Nagaraj, M.; Bhuvanesh, N.; Muthusubramanian, S.; Rajagopal, S. Aggregation Induced Emission Characteristics of Maleimide Derivatives. *RSC Adv.* **2013**, *3*, 22246–22252.
- (43) Yuan, W. Z.; Gong, Y.; Chen, S.; Shen, X. Y.; Lam, J. W. Y.; Lu, P.; Lu, Y.; Wang, Z.; Hu, R.; Xie, N.; et al. Efficient Solid Emitters with Aggregation-Induced Emission and Intramolecular Charge Transfer Characteristics: Molecular Design, Synthesis, Photophysical Behaviors, and OLED Application. *Chem. Mater.* **2012**, *24*, 1518–1528.
- (44) Gao, B.-R.; Wang, H.-Y.; Hao, Y.-W.; Fu, L.-M.; Fang, H.-H.; Jiang, Y.; Wang, L.; Chen, Q.-D.; Xia, H.; Pan, L.-Y.; et al. Time-Resolved Fluorescence Study of Aggregation-Induced Emission Enhancement by Restriction of Intramolecular Charge Transfer State. *J. Phys. Chem. B* **2010**, *114*, 128–134.
- (45) Mishra, A.; Chatterjee, S.; Krishnamoorthy, G. Intramolecular Charge Transfer Emission of *trans*-2-[4'-(Dimethylamino)styryl]-benzimidazole: Effect of Solvent and pH. *J. Photochem. Photobiol. A* **2013**, *260*, 50–58.
- (46) Carlotti, B.; Spalletti, A.; Sindler-Kulyk, M.; Elisei, F. Ultrafast Photoinduced Intramolecular Charge Transfer in Push–Pull Distyryl Furan and Benzofuran: Solvent and Molecular Structure Effect. *Phys. Chem. Chem. Phys.* **2011**, *13*, 4519–4528.
- (47) Tsai, H.-Y.; Chen, K.-Y. Synthesis and Optical Properties of Novel Asymmetric Perylenebisimides. *J. Lumin.* **2014**, *149*, 103–111.
- (48) Qin, W.; Baruah, M.; Van der Auweraer, M.; De Schryver, F. C.; Boens, N. Photophysical Properties of Borondipyrromethene Analogues in Solution. *J. Phys. Chem. A* **2005**, *109*, 7371–7384.
- (49) Aldred, M. P.; Li, C.; Zhang, G.-F.; Gong, W.-L.; Li, A. D. Q.; Dai, Y.; Ma, D.; Zhu, M.-Q. Fluorescence Quenching and Enhancement of Vitrifiable Oligofluorenes End-Capped with Tetraphenylethene. *J. Mater. Chem.* **2012**, *22*, 7515–7528.
- (50) Shi, J.; Wu, Y.; Sun, S.; Tong, B.; Zhi, J.; Dong, Y. Tunable Fluorescence Conjugated Copolymers Consisting of Tetraphenylethylene and Fluorene Units: from Aggregation-Induced Emission Enhancement to Dual-channel Fluorescence Response. *J. Polym. Sci., Part A: Polym. Chem.* **2013**, *51*, 229–240.
- (51) Son, S.-K.; Choi, Y.-S.; Lee, W.-H.; Hong, Y.; Kim, J.-R.; Shin, W.-S.; Moon, S.-J.; Hwang, D.-H.; Kang, I.-N. Synthesis and Properties of Phenothiazylene Vinylene-Based Polymers: New Organic Semiconductors for Field-Effect Transistors and Solar Cells. *J. Polym. Sci., Part A: Polym. Chem.* **2010**, *48*, 635–646.
- (52) Zheng, M.; Sun, M.; Li, Y.; Wang, J.; Bu, L.; Xue, S.; Yang, W. Piezofluorochromic Properties of AIE-Active 9,10-Bis(*N*-alkylphenothiazin-3-yl-vinyl-2)anthracenes with Different Lengths of Alkyl Chains. *Dyes Pigm.* **2014**, *102*, 29–34.
- (53) Kuehne, A. J. C.; Mackintosh, A. R.; Pethrick, R. A. β -Phase Formation in a Crosslinkable Poly(9,9-dihexylfluorene). *Polymer* **2011**, *52*, 5538–5542.
- (54) Lee, S. K.; Ahn, T.; Park, J.-H.; Jung, Y. K.; Chung, D.-S.; Parke, C. E.; Shim, H. K. β -Phase Formation in Poly(9,9-di-*n*-octylfluorene) by Incorporating an Ambipolar Unit Containing Phenothiazine and 4-(Dicyanomethylene)-2-methyl-6-[*p*-(dimethylamino)styryl]-4*H*-pyran. *J. Mater. Chem.* **2009**, *19*, 7062–7069.
- (55) Yang, G.-Z.; Wang, W. -Z.; Wang, M.; Liu, T. Side-Chain Effect on the Structural Evolution and Properties of Poly(9,9-dihexylfluorene-alt-2,5-dialkoxybenzene) Copolymers. *J. Phys. Chem. B* **2007**, *111*, 7747–7755.
- (56) Singh, S. P.; Mohapatra, Y. N.; Qureshi, M.; Manoharan, S. S. White Organic Light-Emitting Diodes Based on Spectral Broadening in Electroluminescence due to Formation of Interfacial Exciplexes. *Appl. Phys. Lett.* **2005**, *86*, 113505/1–113505/3.
- (57) Lee, J.; Lee, J.-I.; park, M.-J.; Jung, Y. K.; Cho, N. S.; Cho, H. J.; Hwang, D.-H.; Lee, S.-K.; park, J.-H.; hong, J.; et al. Phenothiazine-*S,S*-dioxide and Fluorene-Based Light-Emitting Polymers: Introduction of e^- -Deficient *S,S*-Dioxide into e^- -Rich Phenothiazine. *J. Polym. Sci., Part A: Polym. Chem.* **2007**, *45*, 1236–1246.

- (58) Lee, P.-I.; Hsu, S. L.-C.; Lin, P. White-Light-Emitting Diodes from Single Polymer Systems Based on Polyfluorene Copolymers with Quinoxaline Derivatives. *Macromolecules* **2010**, *43*, 8051–8057.
- (59) Coropceanu, V.; Cornil, J.; da Silva Filho, D. A.; Olivier, Y.; Silbey, R.; Brédas, J.-L. Charge Transport in Organic Semiconductors. *Chem. Rev.* **2007**, *107*, 926–952.
- (60) Marcus, R. A. On the Theory of Oxidation-Reduction Reactions Involving Electron Transfer. I. *J. Chem. Phys.* **1956**, *24*, 966–978.
- (61) Ran, X. Q.; Feng, J. K.; Ren, A. M.; Li, W. C.; Zou, L. Y.; Sun, C. C. Theoretical Study on Photophysical Properties of Ambipolar Spirobi fluorene Derivatives as Efficient Blue-Light-Emitting Materials. *J. Phys. Chem. A* **2009**, *113*, 7933–7939.
- (62) Hutchison, G. R.; Ratner, M. A.; Marks, T. J. Hopping Transport in Conductive Heterocyclic Oligomers: Reorganization Energies and Substituent Effects. *J. Am. Chem. Soc.* **2005**, *127*, 2339–2350.
- (63) Varathan, E.; Vijay, D.; Vinod Kumar, P. S.; Subramanian, V. Computational Design of High Triplet Energy Host Materials for Phosphorescent Blue Emitters. *J. Mater. Chem. C* **2013**, *1*, 4261–4274.
- (64) Varathan, E.; Vijay, D.; Subramanian, V. Rational Design of Carbazole- and Carbone-Based Ambipolar Host Materials for Blue Electrophosphorescence: A Density Functional Theory Study. *J. Phys. Chem. C* **2014**, *118*, 21741–21754.
- (65) Yin, J.; Zhang, S.-L.; Chen, R.-F.; Ling, Q.-D.; Huang, W. Carbazole Endcapped Heterofluorenes as Host Materials: Theoretical Study of Their Structural, Electronic, and Optical Properties. *Phys. Chem. Chem. Phys.* **2010**, *12*, 15448–15458.
- (66) Zhang, B.; Qin, C.; Ding, J.; Chen, L.; Xie, Z.; Cheng, Y.; Wang, L. High-Performance All-Polymer White-Light-Emitting Diodes Using Polyfluorene Containing Phosphonate Groups as an Efficient Electron-Injection Layer. *Adv. Funct. Mater.* **2010**, *20*, 2951–2957.